

1. Introduction

Lateral inhibitory networks (LINs) of neurons are thought to be widely used throughout the nervous system and are known to enhance spatial edges and peaks in their input excitation patterns. It is postulated, based on experimental findings (e.g., Suga, 1995), that lateral inhibition contributes to the central, sub-cortical, auditory processing of incident sound. Previous LIN models of the central processing of auditory nerve activity were based on highly simplified phenomenological models of neural activity (Gerken, 1996; Kral and Majernik, 1996; Shamma, 1985). A more biologically realistic model of an auditory LIN has thus been developed to investigate the plausibility of such networks in these central pathways. In particular, the effects on abnormal spontaneous input edges and neural representations of speech, and of peripheral hearing impairment are investigated.

2. The Model

A single layer, uniform, recurrent LIN structure was modeled (Figure 1). Each neuron in the LIN is described by a conductance-based (Figure 2), leaky integrate-and-fire model (Equation 1). Each neuron only receives excitation from a single input spike train. However, inhibitory input is received from the six neighbouring neurons on each side, with each side having Gaussian-shaped inhibitory weights. Input spike instances were obtained from Bruce and colleagues' (2003) model of the auditory periphery for speech sounds and by using the Bernoulli approximation of a Poisson process to represent spontaneous activity from the auditory nerve.

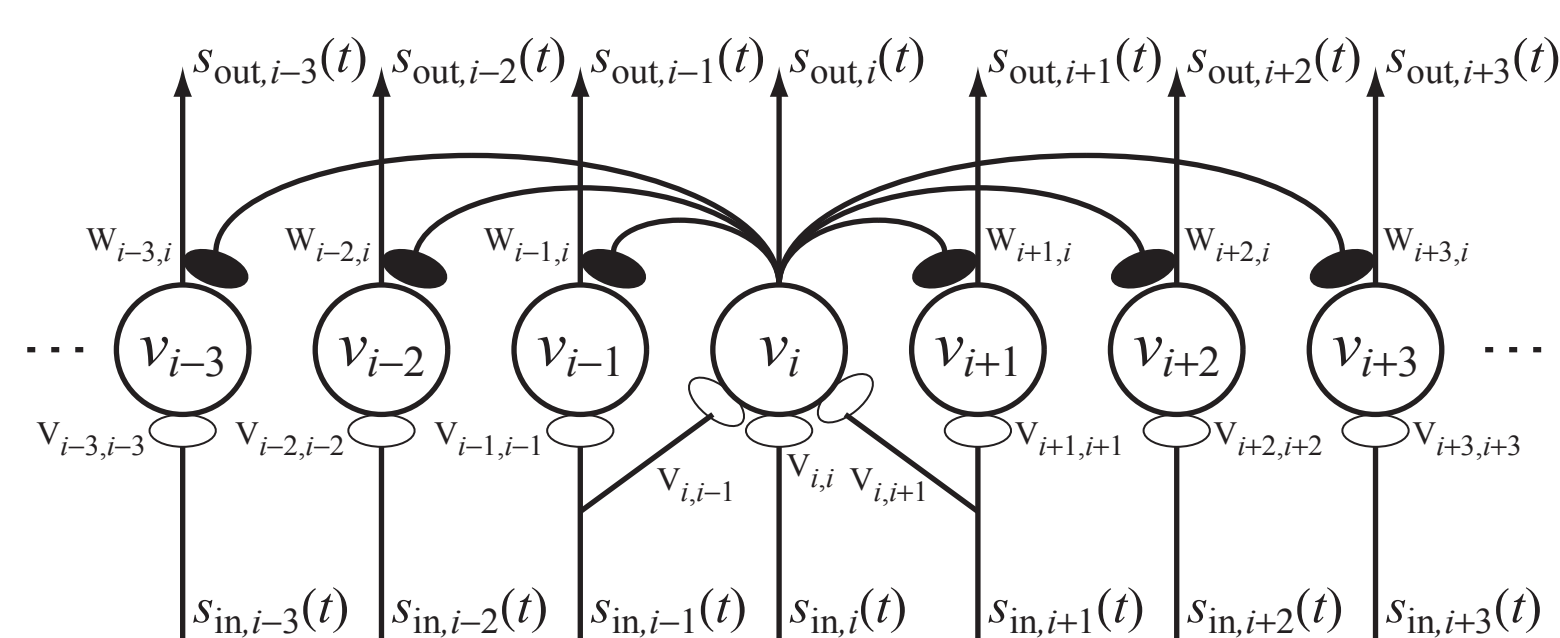


Figure 1: Schematic of a recurrent LIN. Excitatory synaptic inputs are shown by open ellipses and inhibitory synaptic inputs by filled ellipses. Input, $s_{in,i}(t)$, and output, $s_{out,i}(t)$, spike occurrences are convolved with unitary synaptic conductances (see Figure 2) to produce excitatory, $g_{synE}(t)$, and inhibitory, $g_{synI}(t)$, time varying synaptic conductances. V_j and W_{ij} are excitatory and inhibitory synaptic weights. v_i represents the membrane potential of neuron i .

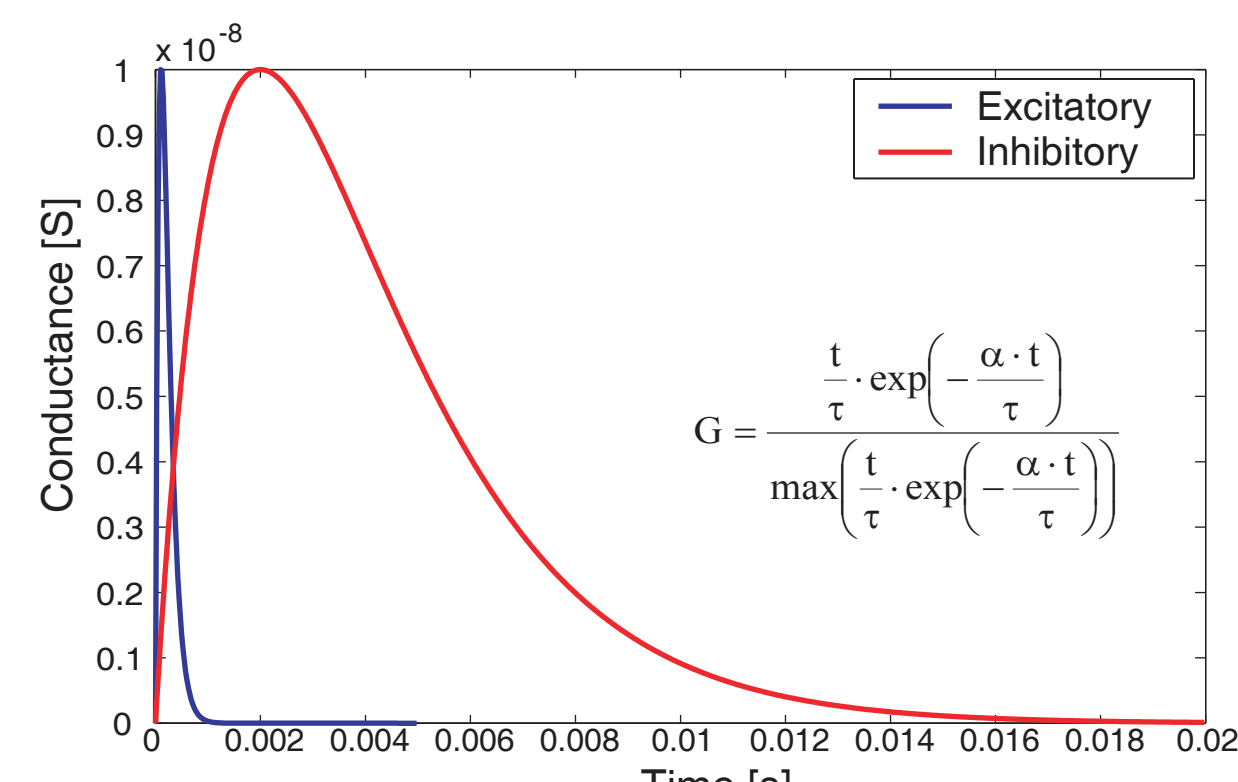


Figure 2: Unitary Excitatory and Inhibitory Conductances

$$\frac{dv(t)}{dt} = \frac{V \cdot g_{synE}(t) \cdot (E_{synE} - v(t)) + W \cdot g_{synI}(t) \cdot (E_{synI} - v(t))}{C} - \frac{v(t)}{\tau}$$

Equation 1: Subthreshold membrane potential

3. Results

The characteristic edge-effect of lateral inhibition that can be seen in the mean spike rates results from a spatial edge at a regional reduction of spontaneous input. The effect of neuronal parameters on the prominence of the spurious peak was measured (Equations 2 & 3; Figures 3 to 8). It was found that the values of the neuronal parameters must fall within a very specific and narrow range for the edge-effect to be seen.

Synthesized speech (Figure 9) processed by Bruce and colleagues' model of the normal and impaired ear was also presented as input to a LIN. The LIN parameters that produced the greatest edge-effect in the spontaneous input simulations were used in this LIN in an effort to maximize any edge enhancement that might occur. To ascertain how formants (vocal tract resonances) in the speech-driven input are affected by this LIN, spatio-temporal response patterns were observed (Figure 10) and power ratios (Equations 4 & 5; Figure 10) (Miller et al., 1997) were used to measure the synchrony of the output of the LIN to the formant frequencies. It was found that the LIN significantly reduces synchrony to the formant frequencies and alters the spatio-temporal response pattern such that the neural representation of speech is degraded. No enhancements were observed.

Equation 2 Peak Height = Peak - Highspont

Equation 3 $EEIndex = \frac{Peak\ Height}{Highspont \cdot (Highspont - Lowspont)}$

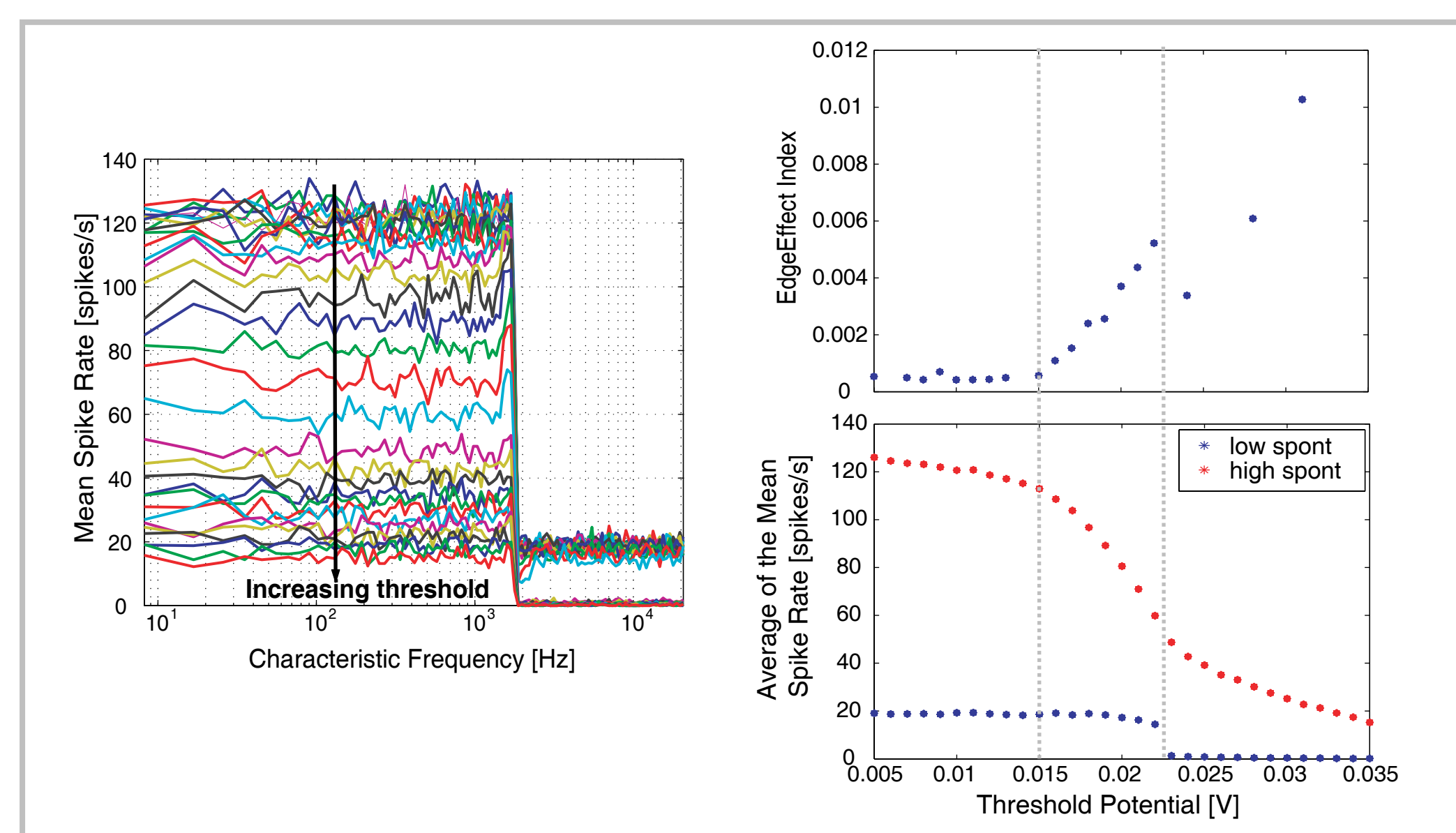


Figure 3: Varying Threshold Potential. Spontaneous input rates of 200 and 20 spikes/s to simulate normal (below 1.6kHz) and impaired (above 1.6kHz) bands of hearing were used. A network of 100 neurons with a membrane time constant of 1ms, capacitance of 7.5nF, refractory period of 2ms, lateral inhibition factor of 2, excitatory and inhibitory reversal potentials of 100mV and -20mV relative to the resting potential, and alpha values of 3 and 10 for inhibitory and excitatory conductances respectively, was modeled. The threshold potential was varied from 5 to 35mV.

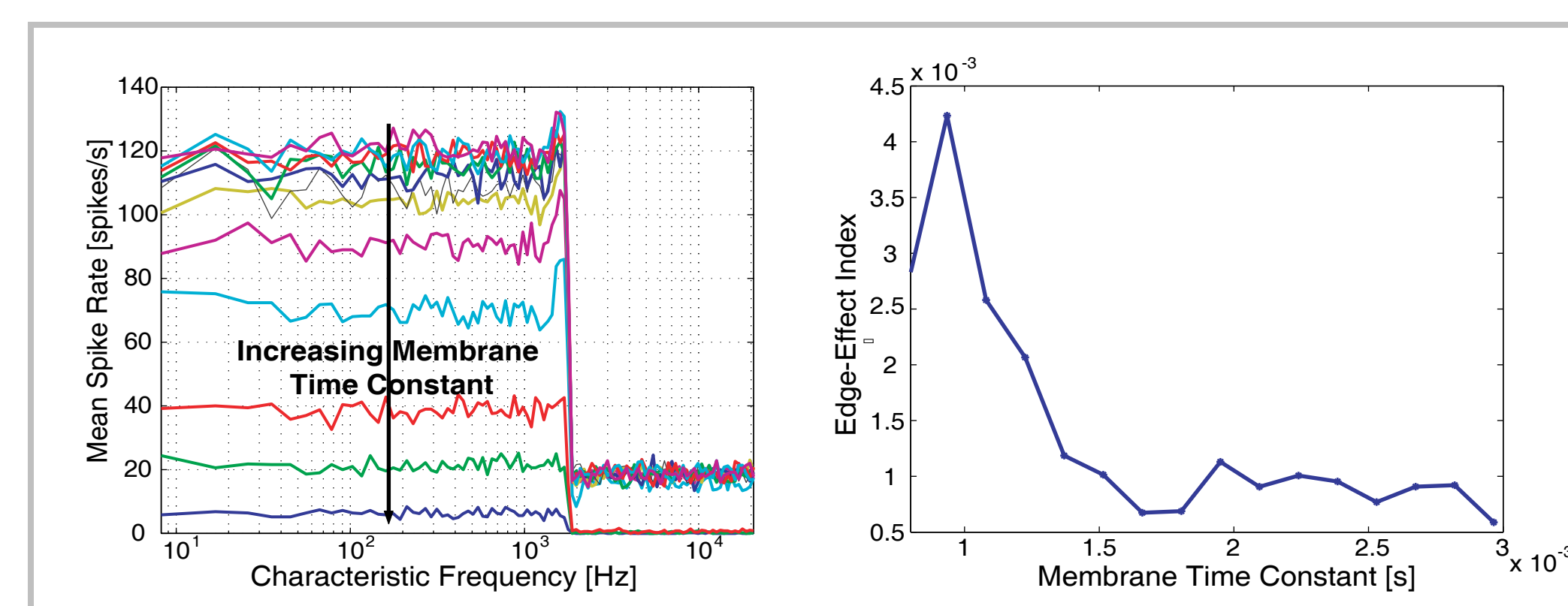


Figure 4: Varying Membrane Time Constant. The same input and neural network parameters as in Figure 3 were used, except that the threshold potential was set at 20mV and the membrane time constant was varied from 0.5 to 3ms.

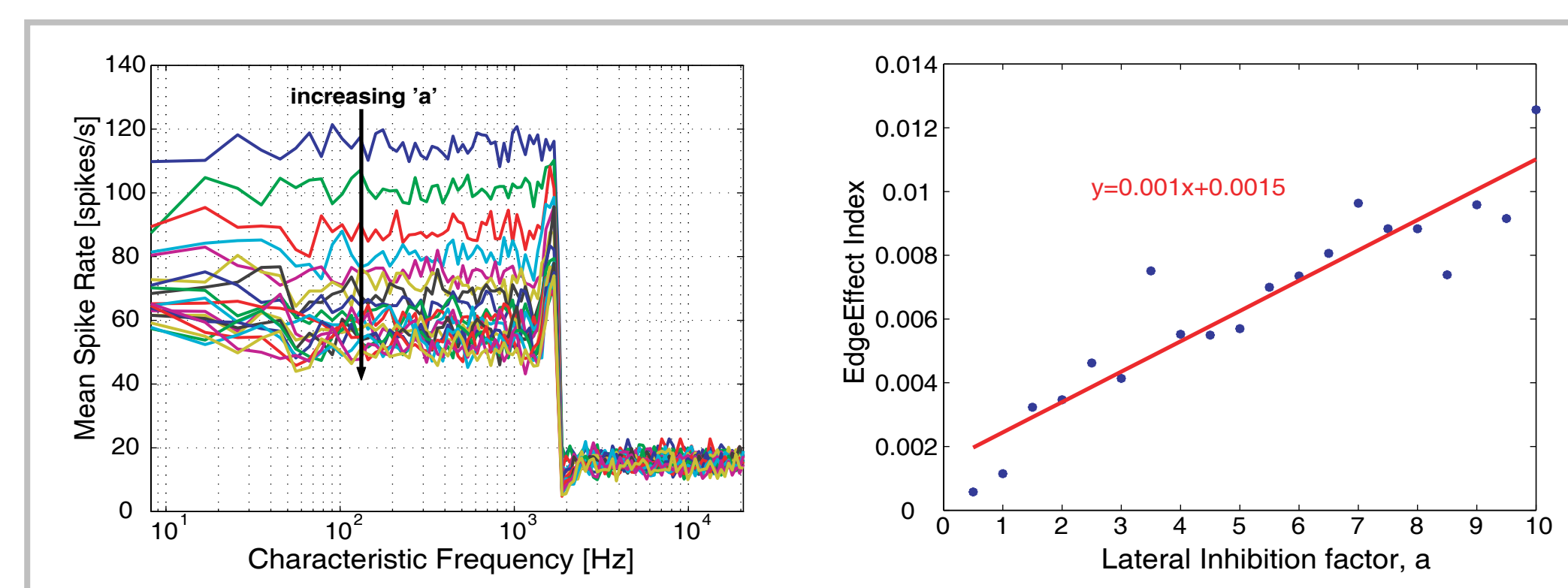


Figure 5: Varying Lateral Inhibition Factor, a. The same input and neural network parameters as in Figure 3 were used, except that the threshold potential was set at 20mV and the lateral inhibition factor was varied from 0.5 to 10.

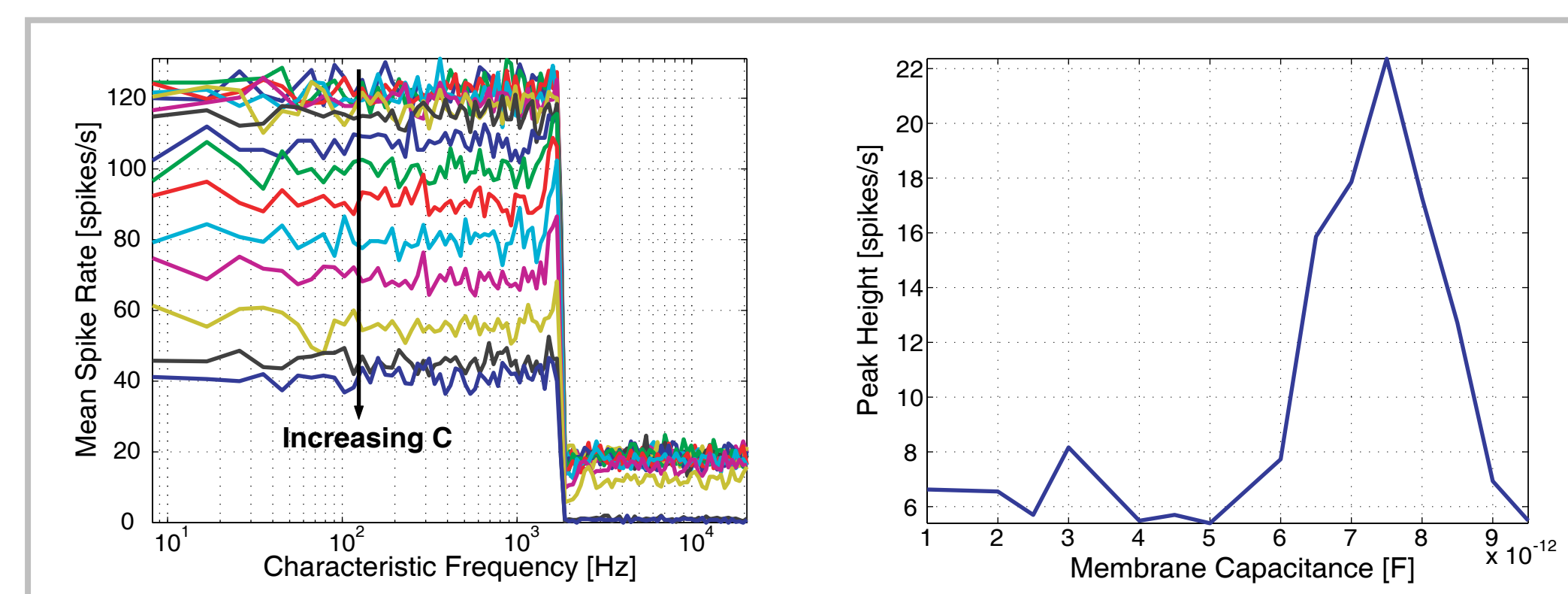


Figure 6: Varying Membrane Capacitance. The same input and neural network parameters as in Figure 3 were used, except that the threshold potential was set at 20mV and the membrane capacitance was varied from 1 to 9.5nF.

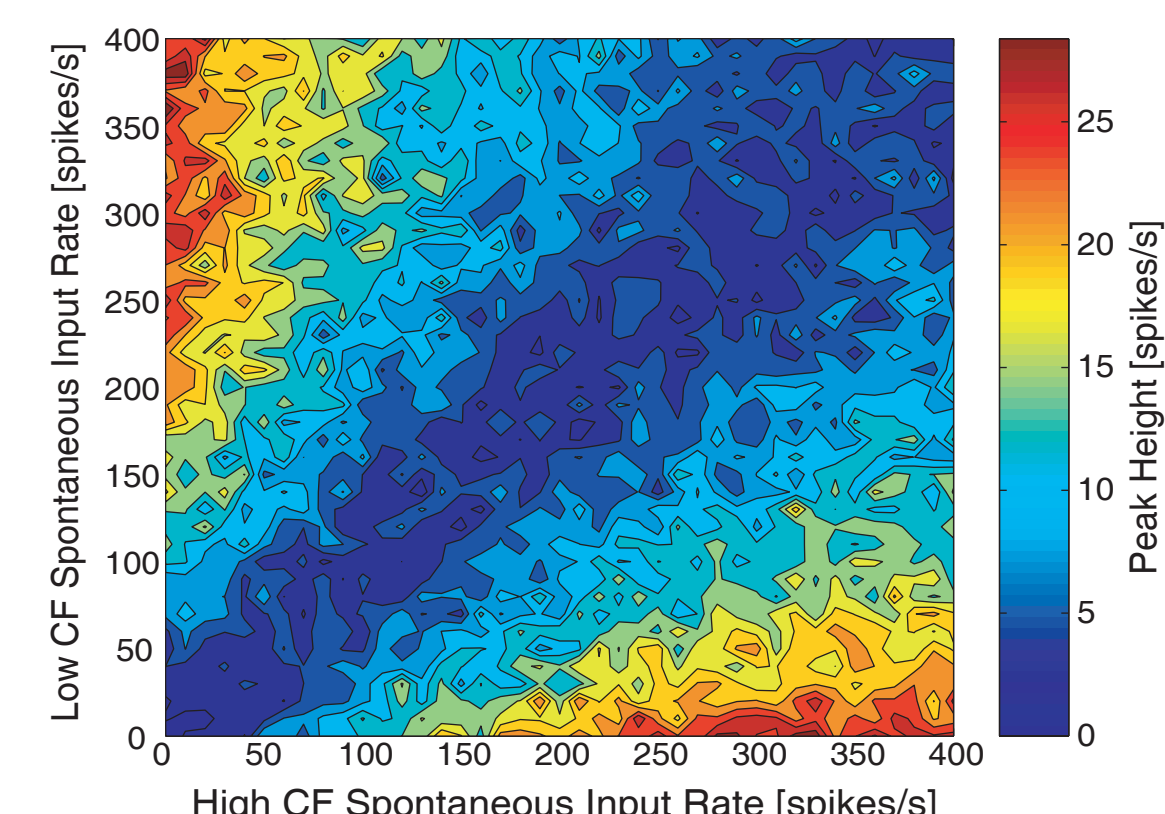


Figure 7: Varying Spontaneous Input Rates. The same neural network parameters as in Figure 3 were used, except that the threshold potential was set at 20mV. The high and low frequency spontaneous input rates were varied from 0 to 400 spikes/s.

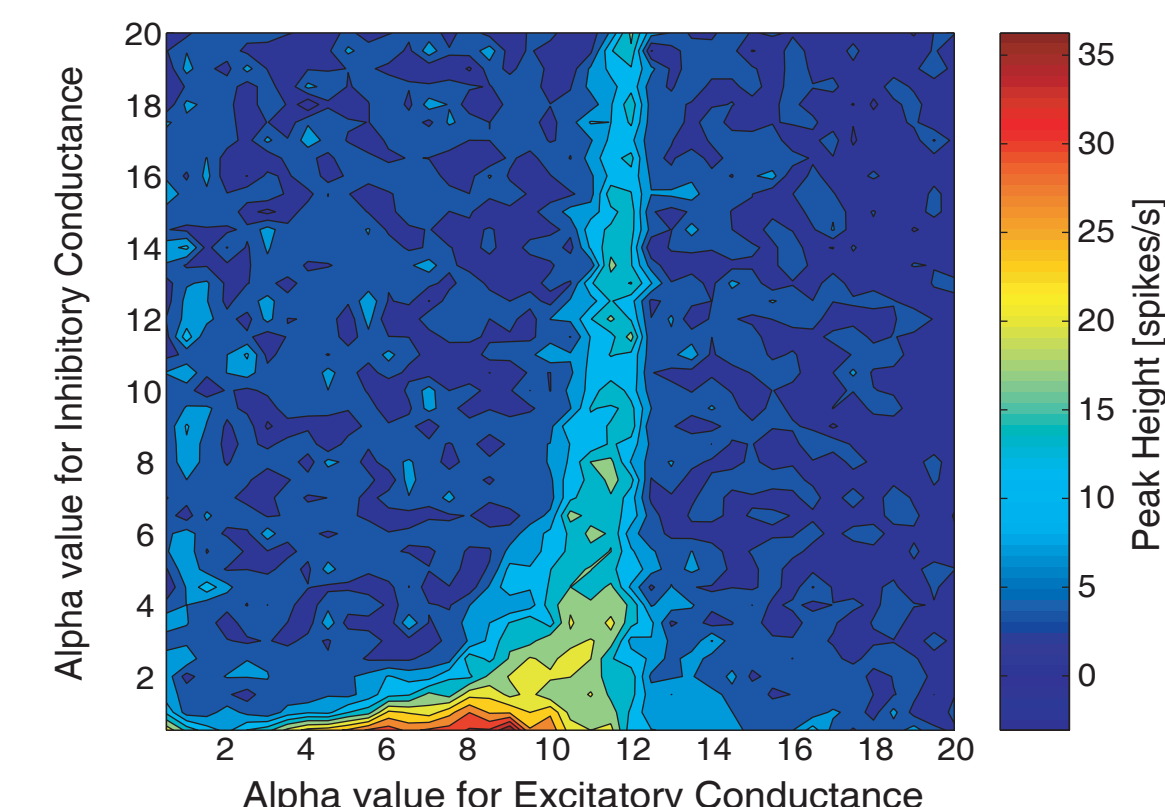


Figure 8: Varying Alpha Values of Conductances. The same input and neural network parameters as in Figure 3 were used, except that the threshold potential was set at 20mV and the alpha values were varied from 0.5 to 20.

Funded by the Canadian Institutes of Health Research (New Emerging Teams grant 54023).

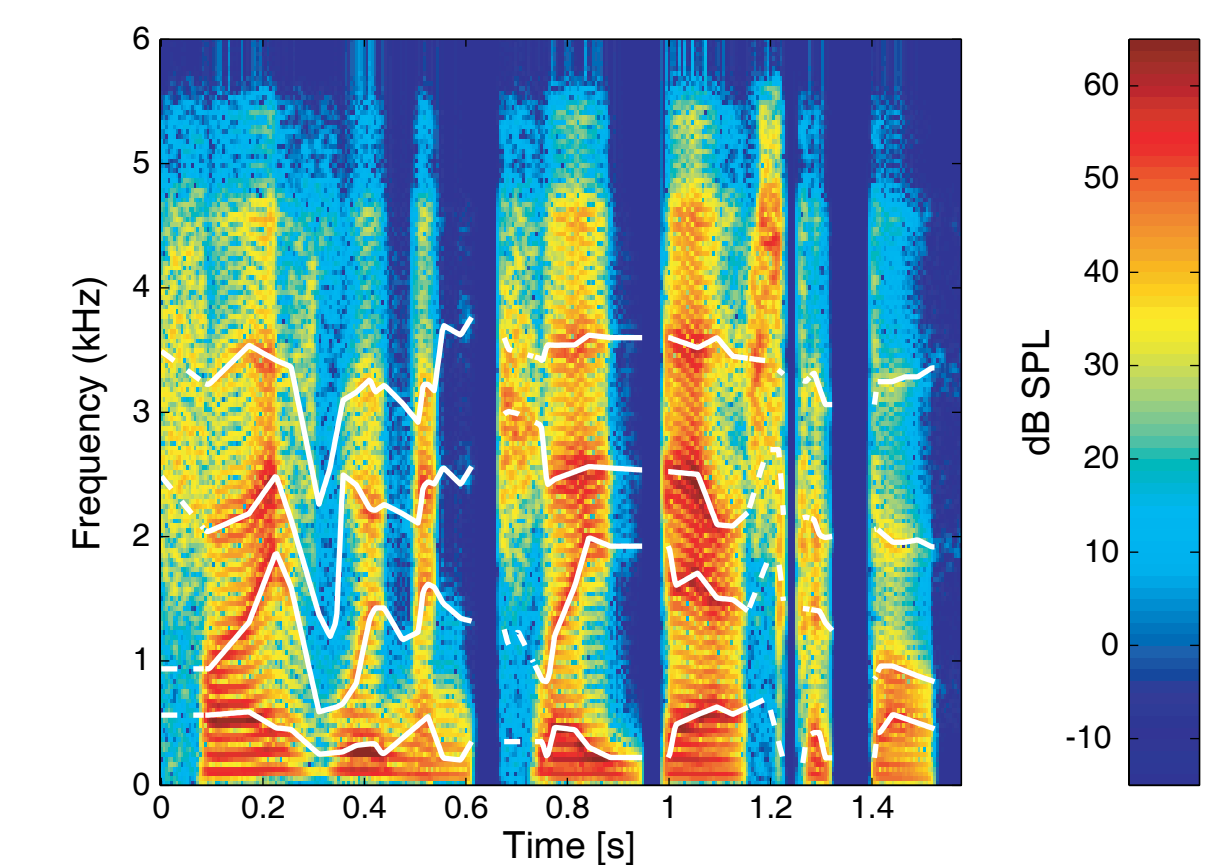


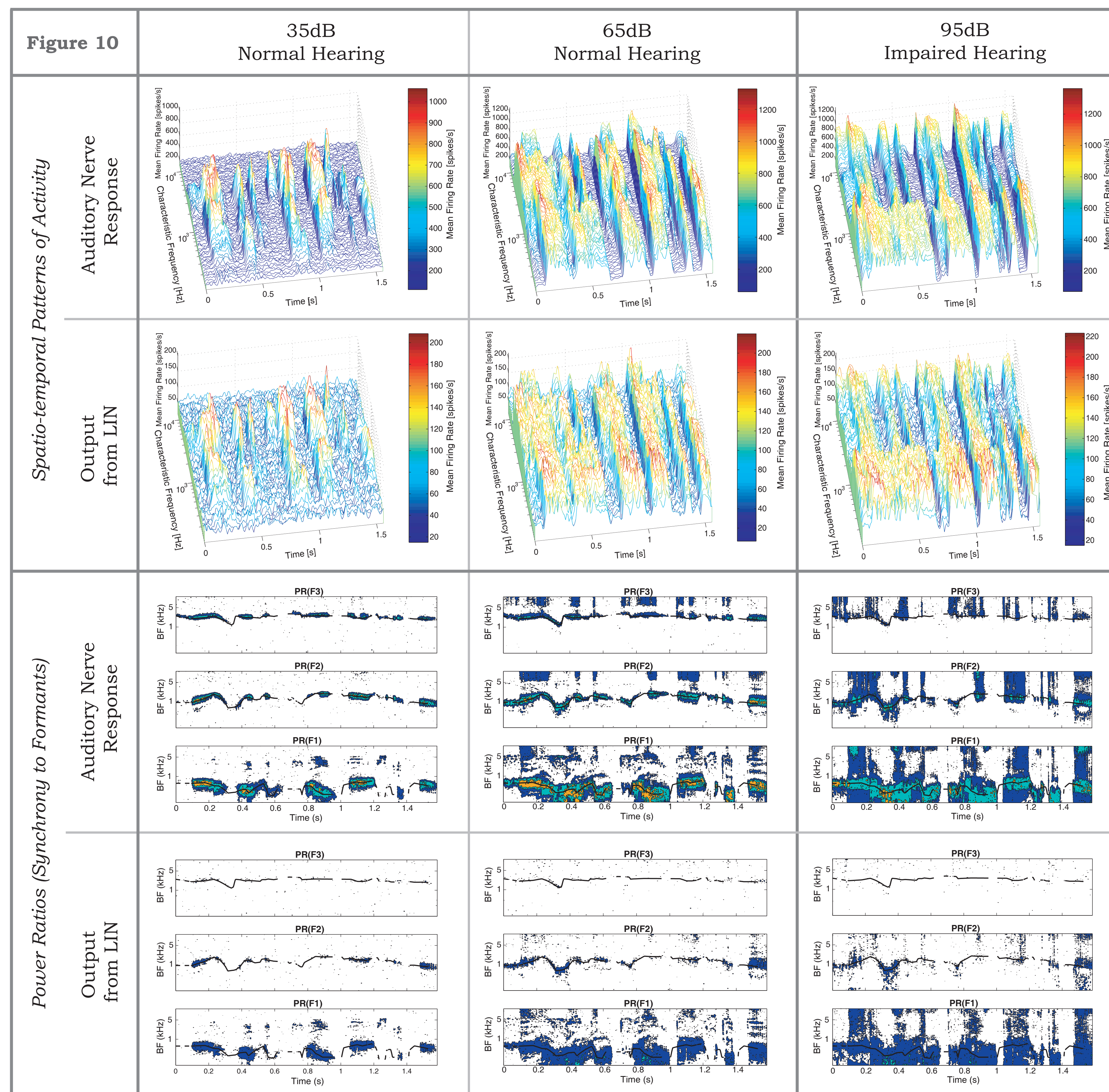
Figure 9: Spectrogram of Synthesized Speech. Male speaker saying "Five women played basketball," presented at 65dB SPL.

$$R(kf_i) = \frac{\sum_{n=0}^{N-1} w(n)p(n)e^{-j2\pi kfn}}{\sqrt{\sum_{n=0}^{N-1} w(n)^2}}$$

Equation 4: Synchronized Rate

$$PR(F_x) = \frac{\sum_{m=1}^M R^2(m \cdot F_x)}{\sum_{n=1}^N R^2(n \cdot F_0)}$$

Equation 5: Power Ratio



4. Discussion and Conclusions

A spurious peak in the output excitation pattern of the LIN may be a neural generator of tinnitus, the phantom perception of sound. Since it was found that a spurious peak could be generated by a LIN whose parameters fall within a specific range, it is possible that a LIN contributes to a central mechanism of tinnitus. However, the feasibility of such a mechanism remains to be determined from anatomical and physiological studies of LINs in the central auditory system.

For LIN processing of speech, harmonics, formants and other patterns that were enhanced by a non-spiking model (Shamma, 1985) were degraded by this spiking model. This result serves as a good example of the importance of the level to which biologically relevant details need to be incorporated into computational models. Although it may be concluded that edge enhancement in complex sounds such as speech may not be realized by recurrent lateral-inhibitory-networks of spiking neurons alone, these results do not preclude the plausibility of other types of neural circuits from doing so.

References

- [1] Shamma SA. Speech processing in the auditory system II: Lateral inhibition and the central processing of speech evoked activity in the auditory nerve. J. Acoust. Soc. Am. 78:1622-1632, 1985.
- [2] Gerken GM. Central tinnitus and lateral inhibition. Hear. Res. 97:75-83, 1996.
- [3] Kral A, Majernik V. On lateral inhibition in the auditory system. Gen. Physiol. Biophys. 15:109-127, 1996.
- [4] Bruce IC, Sachs MB, Young ED. An auditory-periphery model of the effects of acoustic trauma on auditory nerve responses. J. Acoust. Soc. Am. 113:396-388, 2003.
- [5] Suga N. Sharpening of frequency tuning by inhibition in the central auditory system: tribute to Yasuji Katsuki. Neuroscience Research 21:287-299, 1995.
- [6] Miller RL, Schilling JR, Franck KR, Young ED. J. Acoust. Soc. Am. 101(6):3602-3616, 1997.